

# HHT method for system identification and damage detection: an experimental study

Lily L. Zhou<sup>†</sup> and Gang Yan<sup>‡</sup>

College of Aerospace Engineering, Nanjing University of Aeronautics and Astronautics,  
Nanjing 210016, China

(Received April 7, 2005, Accepted January 9, 2006)

**Abstract.** Recently, the Hilbert-Huang transform (HHT) has gained considerable attention as a novel technique of signal processing, which shows promise for the system identification and damage detection of structures. This study investigates the effectiveness and accuracy of the HHT method for the system identification and damage detection of structures through a series of experiments. A multi-degree-of-freedom (MDOF) structural model has been constructed with modular members, and the columns of the model can be replaced or removed to simulate damages at different locations with different severities. The measured response data of the structure due to an impulse loading is first decomposed into modal responses using the empirical mode decomposition (EMD) approach with a band-pass filter technique. Then, the Hilbert transform is subsequently applied to each modal response to obtain the instantaneous amplitude and phase angle time histories. A linear least-square fit procedure is used to identify the natural frequencies and damping ratios from the instantaneous amplitude and phase angle for each modal response. When the responses at all degrees of freedom are measured, the mode shape and the physical mass, damping and stiffness matrices of the structure can be determined. Based on a comparison of the stiffness of each story unit prior to and after the damage, the damage locations and severities can be identified. Experimental results demonstrate that the HHT method yields quite accurate results for engineering applications, providing a promising tool for structural health monitoring.

**Keywords:** Hilbert-Huang transform (HHT); system identification; damage detection; empirical mode decomposition (EMD); experimental study.

---

## 1. Introduction

The need for a rapid assessment of the state of civil infrastructures, including bridges, buildings and others, has been demonstrated during many recent earthquakes and other natural disasters. Thus developing structural health monitoring system (SHMS) that can continuously monitor the structure and reliably respond to any structural anomalies presents new challenges for the civil engineering research community (e.g. Chang 1997, 1999, 2001, 2003, Housner, *et al.* 1997). Different system identification approaches for structural health monitoring and damage detection of civil engineering structures have been proposed in the past years (e.g. Doebling, *et al.* 1996, Dyke, *et al.* 2000, Feldman 1994, 1997, Gurley and Kareem 1999, Hou, *et al.* 2000, Ruzzene, *et al.* 1997, Staszewski 1997), however, to effectively extract damage features from measured data using signal processing techniques is still a challenging task.

---

<sup>†</sup>Professor, Corresponding Author, E-mail: [lzhou@nuaa.edu.cn](mailto:lzhou@nuaa.edu.cn)

<sup>‡</sup>Graduate Research Assistant, E-mail: [yangang@nuaa.edu.cn](mailto:yangang@nuaa.edu.cn)

Recently, a method of decomposing a signal in the time-frequency domain using Hilbert transform has been proposed by Huang, *et al.* (1998, 1999). This method is to decompose the signal into intrinsic mode functions (IMFs) using empirical mode decomposition (EMD) method, where each IMF admits a well-behaved Hilbert transform. Then the Hilbert transform is applied to each intrinsic mode function to obtain a decomposition of the signal in the time-frequency domain. Such a process is referred to as the Hilbert-Huang transform (HHT). The HHT method has been widely applied to different research fields, such as speech, machine health monitoring, bio-medical data analysis, etc. In the preliminary studies, a method based on the EMD and Hilbert transform has been proposed and applied to identify the modal parameters of multi-degree-of-freedom (MDOF) linear structures, including natural frequencies and damping ratios (Yang and Lei 1999). This method was demonstrated to be capable of identifying modal parameters more accurately than the method of wavelet transform (WT), when the natural frequencies are close to each other (Ruzzene 1997). The method was extended later to identify not only the natural frequencies and damping ratios, but also the mode shapes, the mass, stiffness and damping matrices of linear structures in which the mode shapes may be real or complex, thus showing a great promise for structural health monitoring (Yang, *et al.* 2000, 2001, 2002, 2003a, 2003b).

For the method of system identification based on HHT proposed by Yang, *et al.* (2003a, 2003b), free vibration measurements polluted by noises are used. The measured signals of MDOF linear systems are first decomposed into the modal responses using the EMD approach and appropriate intermittency criteria. Depending on the frequencies of the system, a filtering technique may be used in conjunction with the EMD method. A modal response thus obtained is a special IMF that admits well-behaved Hilbert transform. The Hilbert transform is then applied to each modal response to obtain the instantaneous phase angle and amplitude as functions of time  $t$ . Then, a linear least-square fit algorithm is proposed to fit the instantaneous phase angle and the log of instantaneous amplitude. From the slopes of these linear least-square lines, the natural frequency and damping ratio for each mode can be identified. Based on a single measurement of the free vibration time history at one appropriate location of the MDOF linear system, all natural frequencies and damping ratios can be identified. When the responses at all degrees of freedom are measured, the complete system dynamic characteristics can all be identified, including the mode shapes and physical mass, damping and stiffness matrices. Likewise, the HHT method has been applied to a benchmark problem for the determination of structural damages (Yang, *et al.* 2004).

This study investigates the effectiveness and accuracy of the HHT method for system identification and damage detection through a series of experiments. A MDOF structural model was constructed with modular members, and the columns can be replaced or removed to simulate damages at different locations with different severities. The physical mass, damping and stiffness matrices were successfully identified from the measured structural responses using the HHT method. By comparing the stiffness of each story unit before and after damages, the location and severity of the damage were accurately determined.

## 2. Theoretical foundation

### 2.1. Modal response of MDOF structures due to impulse loading

Generally speaking, all the eigenvalues and eigenvectors of linear structures are complex, hence, complex modes rather than normal modes are considered in this study (Yang, *et al.* 2003b). The equation of motion of a general  $n$ -DOF structure can be expressed as

$$\mathbf{M}\ddot{\mathbf{X}}(t) + \mathbf{C}\dot{\mathbf{X}}(t) + \mathbf{K}\mathbf{X}(t) = \mathbf{F}(t) \quad (1)$$

in which  $\mathbf{X}(t) = [x_1, x_2, \dots, x_n]^T = n$ -displacement vector,  $\mathbf{F}(t) = n$ -excitation vector, and  $\mathbf{M}$ ,  $\mathbf{C}$  and  $\mathbf{K}$  are ( $n \times n$ ) mass, damping and stiffness matrices, respectively. In the state-space, Eq. (1) can be expressed as

$$\mathbf{A}\dot{\mathbf{Y}} + \mathbf{B}\mathbf{Y} = \mathbf{G} \text{ or } \dot{\mathbf{Y}} = \mathbf{D}\mathbf{Y} + \mathbf{A}^{-1}\mathbf{G} \quad (2)$$

in which  $\mathbf{Y} = [x_1, x_2, \dots, x_n, \dot{x}_1, \dot{x}_2, \dots, \dot{x}_n]^T$  is a  $2n$  state vector and

$$\mathbf{Y} = \begin{Bmatrix} \mathbf{X} \\ \dot{\mathbf{X}} \end{Bmatrix}, \mathbf{A} = \begin{bmatrix} \mathbf{C} & \mathbf{M} \\ \mathbf{M} & \mathbf{0} \end{bmatrix}, \mathbf{B} = \begin{bmatrix} \mathbf{K} & \mathbf{0} \\ \mathbf{0} & -\mathbf{M} \end{bmatrix}, \mathbf{G} = \begin{Bmatrix} \mathbf{F} \\ \mathbf{0} \end{Bmatrix}$$

$$\mathbf{D} = -\mathbf{A}^{-1}\mathbf{B} = \begin{bmatrix} \mathbf{0} & \mathbf{I} \\ -\mathbf{M}^{-1}\mathbf{K} & -\mathbf{M}^{-1}\mathbf{C} \end{bmatrix} \quad (3)$$

Complex eigenvalues  $\lambda_j$  and eigenvectors  $\Psi_j$  can be obtained from the system matrix  $\mathbf{D}$  as

$$\mathbf{D}\Psi_j = \lambda_j\Psi_j; \quad j = 1, 2, \dots, 2n \quad (4)$$

in which eigenvalues and eigenvectors are all in complex conjugate pairs, and

$$\Psi_j = \begin{Bmatrix} \Phi_j \\ \lambda_j\Phi_j \end{Bmatrix} \quad (5)$$

where  $\Phi_j$  is an  $n$  complex vector.

The response of the state vector can be expressed as

$$\mathbf{Y} = \Psi\mathbf{q} = \sum_{j=1}^{2n} \Psi_j q_j(t) \quad (6)$$

in which  $\mathbf{q}$  is the generalized modal coordinate vector with the  $j$ -th complex element  $q_j(t)$ . Using the orthogonal properties of complex mode shapes, and substituting Eq. (6) into Eq. (2), one obtains the decoupled equations from Eq. (2) as

$$a_j\dot{q}_j + b_jq_j = \Psi_j^T\mathbf{G} \quad (7)$$

in which

$$a_j = \Psi_j^T\mathbf{A}\Psi_j; \quad b_j = \Psi_j^T\mathbf{B}\Psi_j; \quad \lambda_j = -b_j/a_j; \quad j = 1, 2, \dots, 2n \quad (8)$$

The acceleration response of the structure can be expressed as

$$\ddot{\mathbf{X}} = \Phi\ddot{\mathbf{q}} = \sum_{j=1}^{2n} \Phi_j\ddot{q}_j(t) \quad (9)$$

When an impact loading  $F_0 \delta(t)$  is applied to the  $k$ -th DOF, the responses  $q_j(t)$  and  $\ddot{q}_j(t)$  can be obtained from Eq. (7) and Eq. (8) as

$$q_j(t) = \frac{F_0 \phi_{kj}}{a_j} e^{\lambda_j t}; \quad \ddot{q}_j(t) = B_{kj} e^{\lambda_j t} \quad (10)$$

where  $\phi_{kj}$  is the  $k$ -th element of  $\Phi_j$  and

$$B_{kj} = \frac{F_0 \lambda_j^2 \phi_{kj}}{a_j} \quad (11)$$

Eigenvalues  $\lambda_j$  and eigenvectors  $\Psi_j$  as well as  $a_j$ ,  $b_j$ ,  $q_j(t)$  and  $\ddot{q}_j(t)$  are all  $n$  pairs of complex conjugates, e.g.,

$$\lambda_j = -\xi_j \omega_j + i \omega_{dj}; \quad \lambda_{n+j} = \lambda_j^* = -\xi_j \omega_j - i \omega_{dj}; \quad j = 1, 2, \dots, n \quad (12)$$

where  $i = \sqrt{-1}$ ,  $\omega_j = j$ -th modal frequency,  $\xi_j = j$ -th modal damping ratio, and  $\omega_{dj} = \omega_j(1 - \xi_j^2)^{1/2}$ .

The acceleration response  $\ddot{x}_p(t)$  of the structure at  $p$  ( $p = 1, 2, \dots, n$ ) DOF can be expressed as

$$\ddot{x}_p(t) = \sum_{j=1}^{2n} \phi_{pj} \ddot{q}_j(t) = \sum_{j=1}^{2n} \phi_{pj} B_{kj} e^{\lambda_j t} = \sum_{j=1}^n \ddot{x}_{pj}(t) \quad (13)$$

where  $x_{pj}(t)$  is the  $j$ -th modal response given by

$$\ddot{x}_{pj}(t) = R_{pj,k} e^{-\xi_j \omega_j t} \cos[\omega_{dj} t + \theta(\phi_{pj}) + \theta(B_{kj})] \quad (14)$$

$$R_{pj,k} = 2 |\phi_{pj}| |B_{kj}| \quad (15)$$

In Eqs. (14) and (15),  $\theta(\phi_{pj})$  and  $\theta(B_{kj})$  are phase angles of the complex quantities  $\phi_{pj}$  and  $B_{kj}$ , respectively, and  $|\phi_{pj}|$  and  $|B_{kj}|$  are their corresponding amplitudes.

## 2.2. Determination of modal response using EMD method

In real engineering application, the measured acceleration response vector  $\ddot{\mathbf{Z}}(t) = [\ddot{z}_1(t), \ddot{z}_2(t), \dots, \ddot{z}_n(t)]^T$  is polluted by noise, i.e.,

$$\ddot{\mathbf{Z}}(t) = \ddot{\mathbf{X}}(t) + \ddot{\mathbf{V}}(t) \quad (16)$$

where  $\mathbf{V}(t) = [v_1(t), v_2(t), \dots, v_n(t)]^T$  is a white noise vector in which each element, say  $v_p(t)$ , can be modeled as a band-limited Gaussian white noise process. The measured acceleration response  $\ddot{z}_p(t)$  at the  $p$ -th DOF is given by

$$\ddot{z}_p(t) = \ddot{x}_p(t) + v_p(t) = \sum_{j=1}^n \ddot{x}_{pj}(t) + v_p(t) \quad (17)$$

in which  $\ddot{x}_{pj}(t)$  is given by Eqs. (14) and (15).

Yang, *et al.* (2003b) presented a method to obtain the modal response  $\ddot{x}_{pj}(t)$  from measured response

$\ddot{z}_p(t)$  by using the empirical mode decomposition (EMD) method. The procedure of EMD is to construct upper and lower envelopes of the signal by spline fitting, and the average (mean) of both envelopes are computed. Then the signal is subtracted from the mean, referred to as the sifting process. By repeating the sifting process until the resulting signal becomes a monocomponent, i.e., one up-crossing (or down-crossing) of zero will result in one local peak (or trough) indicating that the number of up-crossings (or down-crossings) of zero is equal to the number of peaks (or troughs). Such a monocomponent signal admits a well-behaved Hilbert transform and it is referred to as an IMF. The original signal is then subtracted from the IMF, and the repeated sifting process is applied to the remaining signal to obtain another IMF, until the residue is the mean trend (or a constant) of the signal. Such a process is referred as the EMD method (Huang, *et al.* 1998, 1999).

To ensure the IMFs obtained from the sifting process are the modal response  $\ddot{x}_{pj}(t)$ , an intermittency frequency should be imposed during the sifting process in EMD (Yang, *et al.* 2003a, Huang, *et al.* 1998, 1999). However, the numerical computation based on this approach may be quite involved, thus an alternative approach based on a band-pass filter and EMD is proposed to simplify the computation efforts (Yang, *et al.* 2003a). First, from the Fourier spectrum, the approximate frequency range for each natural frequency, i.e.,  $\omega_{jL} < \omega_j < \omega_{jH}$  ( $j = 1, 2, \dots, n$ ), is determined, where  $\omega_{jL}$ ,  $\omega_{jH}$  are the intermittency frequencies. Then, the measured signal  $\ddot{z}_p(t)$  can be processed through the band-pass filters each with a frequency band  $\omega_{jL} < \omega_j < \omega_{jH}$ . The time history obtained from the  $j$ th band-pass filter is then processed through EMD, and the resulting first IMF is quite close to the  $j$ th modal response. Repeating the same processes for ( $j = 1, 2, \dots, n$ ), one obtains  $n$  modal responses. Thus,  $\ddot{z}_p(t)$  can be decomposed into  $n$  modal response functions (that are also IMFs),  $m-n$  other IMFs and a residue signal as follows:

$$\ddot{z}_p(t) \approx \sum_{j=1}^n \ddot{x}_{pj}(t) + \sum_{j=1}^{m-n} c_{pj}(t) + r_p(t) \quad (18)$$

This is a simple approach that not only can extract the modal response  $\ddot{x}_{pj}(t)$  easily, but also can remove all the noises outside the frequency range. This approach will be used in the experimental study to obtain the modal responses.

### 2.3. System identification of linear structure based on HHT method

As aforementioned, the IMF obtained by the EMD method admits a well-behaved Hilbert transform. By taking the Hilbert transform of  $\ddot{x}_{pj}(t)$  in Eq. (14) and forming the analytical signal

$$Y_{pj}(t) = \ddot{x}_{pj}(t) + \underline{i} \tilde{\ddot{x}}_{pj}(t) = A_{pj}(t) e^{\underline{i} \theta_{pj}(t)} \quad (19)$$

where  $\tilde{\ddot{x}}_{pj}(t)$  is the Hilbert transform of  $\ddot{x}_{pj}(t)$ , the instantaneous amplitude  $A_{pj}(t)$  and phase angle  $\theta_{pj}(t)$  of the signal can be obtained. The details of the theory of Hilbert transform and the Hilbert transform of modal responses are available in many references (Huang, *et al.* 1998, 1999, Yang, *et al.* 2003a, 2003b).

When the damping ratio  $\xi_j$  is very small, one obtains (Yang, *et al.* 2003a, 2003b).

$$\tilde{\ddot{x}}_{pj}(t) \approx R_{pj,k} e^{-\xi_j \omega_j t} \sin(\omega_{dj} t + \theta(\phi_{pj}) + \theta(B_{kj})) \quad (20)$$

$$A_{pj}(t) = R_{pj,k} e^{-\xi_j \omega_j t}; \quad \theta_{pj}(t) = \omega_{dj} t + \theta(\phi_{pj}) + \theta(B_{kj}) \quad (21)$$

It follows from Eq. (21) that

$$\ln A_{pj}(t) = -\xi_j \omega_j t + \ln B_{p_j, k}; \quad \omega_j(t) = d\theta_{pj}(t)/dt = \omega_{dj} \quad (22)$$

It can be seen from Eq. (22) that, for small damping ratio  $\xi_j$ , the damped natural frequency  $\omega_{dj}$  can be obtained from the slope of the phase angle  $\theta_{pj}(t)$  vs. time  $t$  plot, whereas  $-\xi_j \omega_j$  can be estimated from the slope of the decaying amplitude  $\ln A_{pj}(t)$  vs. time  $t$  plot. The linear least square approach can be used to fit the two plots, and hence the natural frequencies and damping ratios can be identified by the slopes of the fitted straight lines. After identifying  $\omega_j$  and  $\xi_j$  for  $j = 1, 2, \dots, n$  the complex eigenvalue  $\lambda_j$  can be computed from Eq. (12).

To identify the complex mode shapes of a structure, the responses at all DOF should be measured. From Eqs. (11), (13) and (22), the ration of the absolute value of modal elements  $\phi_{pj}$  and  $\phi_{qj}$  ( $p, q = 1, 2, \dots, n$ ) of the  $j$ -th mode can be identified as

$$|\phi_{pj}|/|\phi_{qj}| = \exp[A'_{pj}(t_0) - A'_{qj}(t_0)] \quad (23)$$

in which  $A'_{pj}(t_0)$  and  $A'_{qj}(t_0)$  are the magnitudes at time  $t = t_0$  of the least-square straight lines of  $\ln A_{pj}(t)$  and  $\ln A_{qj}(t)$ , respectively. And the difference between the phase angle of the modal element  $\phi_{pj}$  and that of  $\phi_{qj}$  can be expressed as

$$\theta(\phi_{pj}) - \theta(\phi_{qj}) = \theta'_{pj}(t_0) - \theta'_{qj}(t_0) \quad (24)$$

in which  $\theta'_{pj}(t_0)$  and  $\theta'_{qj}(t_0)$  are the magnitudes of the least-square straight lines of the phase angles  $\theta_{pj}(t)$  and  $\theta_{qj}(t)$  at time  $t = t_0$ , respectively. Thus, both the absolute values and phase angles of all modal elements relative to an arbitrary element in the complex modal vector  $\Phi_j$  have been determined. Then, the complex eigenvectors  $\Psi_j$  can be computed from Eq. (5).

The amplitude of the complex value  $a_j$  and phase angle of  $a_j$  can be determined from Eqs. (11), (15) and (22) as

$$|a_j| = \frac{2F_0 |\phi_{pj}| |\phi_{kj}| \lambda_j^2}{\exp[A'_{pj}(0)]}; \quad \theta(a_j) = -\theta_{pj}(0) + \theta(\lambda_j^2) + \theta(\phi_{pj}) + \theta(\phi_{kj}); \quad j = 1, 2, \dots, n \quad (25)$$

in which  $A'_{pj}(0)$  is the magnitude of the least-square straight line of the amplitude  $\ln A_{pj}(t)$  at time  $t = 0$ ,  $F_0$  is the level of impact loading,  $\theta_{pj}(0)$  is the magnitude of the least-square straight line of the phase angle  $\theta_{pj}(t)$  at time  $t = 0$ ,  $\theta(\lambda_j^2)$  is the phase angle of the complex value  $\lambda_j^2$ , and  $\theta(\phi_{pj})$  and  $\theta(\phi_{kj})$  are the phase angles of the complex modal elements  $\theta_{pj}$  and  $\theta_{qj}$ , respectively. Then, the complex value of  $b_j$  can be obtained from Eq. (8) as

$$b_j = -\lambda_j a_j \quad (26)$$

Thus, the mass, damping and stiffness matrices ( $\mathbf{M}$ ,  $\mathbf{C}$ ,  $\mathbf{K}$ ) can be determined using the orthogonal properties of the complex modes in Eqs. (3) and (8).

For damage detection, the assumption is that the damage may cause stiffness reduction while the damping matrices may not change. Therefore, when the system parameters such as mass, stiffness and

damping matrices before and after damages are identified, the damage location and severity can be determined by comparing the identified stiffness matrices.

### 3. Experimental study

#### 3.1. Experimental set-up

To verify the system identification and damage detection methodology based on the HHT method presented above, a series of experiments were conducted in Structure and Strength Laboratory, Nanjing University of Aeronautics and Astronautics.

The overall experimental configuration of this study is shown in Fig. 1. A three-story test structure was constructed and fixed to the ground. The structure is 90 cm tall and has a total mass of 64.6 kg which is distributed uniformly between the floors. The three-story structural model is constructed with modular members, and the columns can be replaced or removed to study the variations in structural parameters. Each floor is supported by 6 steel columns, and the columns are made of the same material, A3 steel, as the distributed mass. The dimension of the column is 16 mm×4 mm×320 mm, and the mass of the columns can be ignored relative to the distributed mass. The stiffness of each story can be computed by using the dimensions of columns and the elastic module of A3 steel, i.e., 216 GPa. This experimental structural model can be considered as a three-story shear-beam type building model and the mass, stiffness of each story unit are identical with  $m_j = 21.53$  kg, and  $k_j = 47619$  N/m, respectively, for  $j = 1, 2, 3$ , which is numbered from bottom to top. However, the damping ratio of each story unit can not be determined at this stage. To experimentally verify the HHT method for system identification and damage detection, columns were removed from the structure to simulate the damage at different location with different severity.

Three PCB20885 accelerometers, whose sensitivity is 100 mV/g, were fixed at the center of each floor to measure the acceleration responses of the structure subject to impulse loadings. Impulse loadings were produced by a PCB086B02 impact hammer. In the experiments, the impulse loading was applied at the middle of the top floor in the x-direction, and only the acceleration responses in the



(a) Baseline Structure

(b) Damage Pattern I

(c) Damage Pattern II

Fig. 1 A MDOF structure for system identification and damage detection

x-direction were measured. The reference coordinate frame in this study is illustrated in Fig. 1(a). A dynamic signal analyzer (HP35670A) was used to acquire the impact loading time history and acceleration responses. The un-damaged structure shown in Fig. 1(a) is referred to as the baseline structure. In this study, two damage patterns were considered. For damage pattern I, two middle columns in the highest story unit were removed to simulate the damage in the top story as shown in Fig. 1(b). For damage pattern II, two middle columns in both the second and the third story units were removed to simulate the damage in both stories as shown in Fig. 1(c).

Further, the finite element method (FEM) has been used to obtain the numerical results of modal parameters for the test structure before and after damage. These finite element results will serve as baselines for comparison with the predictions based on the experimental data.

### 3.2. Experimental results

As mentioned previously, two damage patterns were considered in this study. To verify the accuracy and effectiveness of the HHT method and to provide the baseline information for identifying the location and severity of damages, the baseline structure, namely, the un-damaged structure, was tested and studied first.

Fig. 2 shows the impact force applied to the top floor and the measured acceleration responses of the baseline structure. In this figure,  $\ddot{x}_j$  denotes the measured acceleration response of the  $j$ th floor ( $j = 1, 2, 3$ ). The Fourier transform of the measured signals was performed using the dynamic signal analyzer. Fig. 3 shows the Fourier transform of  $\ddot{x}_3$ . From the figure, it can be observed that there are three dominant frequencies around 3, 9, and 13 Hz, respectively. These acceleration responses were then decomposed into modal responses using the EMD and band-pass filter approaches described in the theoretical part. According to the frequency range obtained from the Fourier transform, the frequency bands of the band-pass filters were taken to be:  $11\text{ Hz} = \omega_{3L} < \omega_3 < \omega_{3H} = 15\text{ Hz}$ , and  $5\text{ Hz} = \omega_{2L} < \omega_2 < \omega_{2H} = 11\text{ Hz}$ , and  $2\text{ Hz} = \omega_{1L} < \omega_1 < \omega_{1H} = 5\text{ Hz}$ , respectively. The filtered time history was then processed through the EMD procedure, and the resulting first IMF was considered as the corresponding  $j$ th modal response. Fig. 4 shows the three modal acceleration responses extracted from  $\ddot{x}_3$ , denoted by

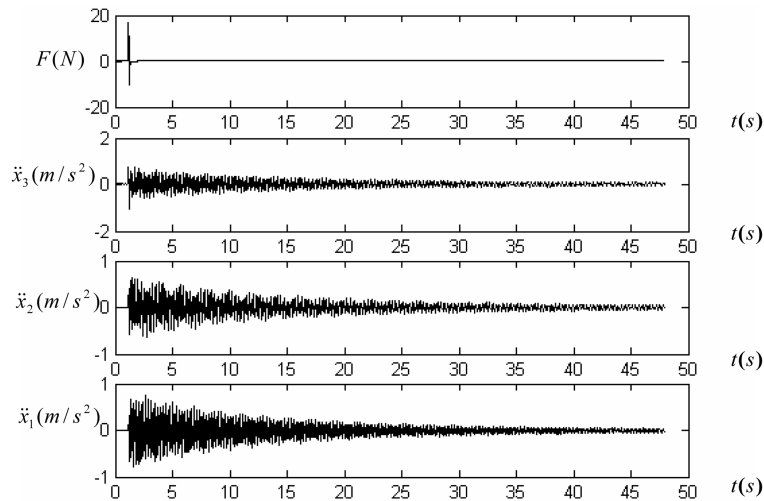


Fig. 2 Time histories of impact force and accelerations of the baseline structure

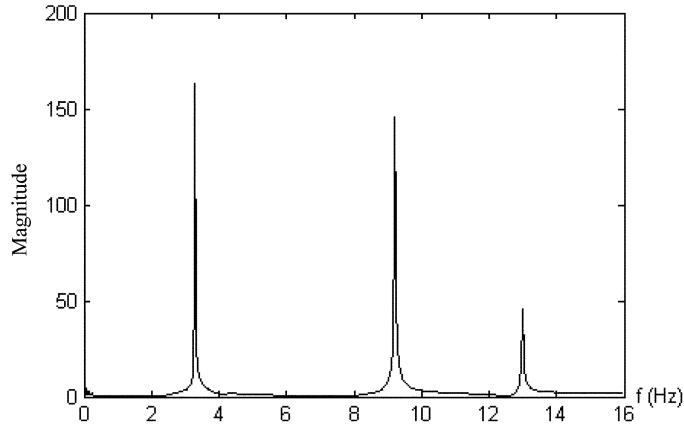


Fig. 3 Fourier transform of acceleration response  $\ddot{x}_3$  of the baseline structure

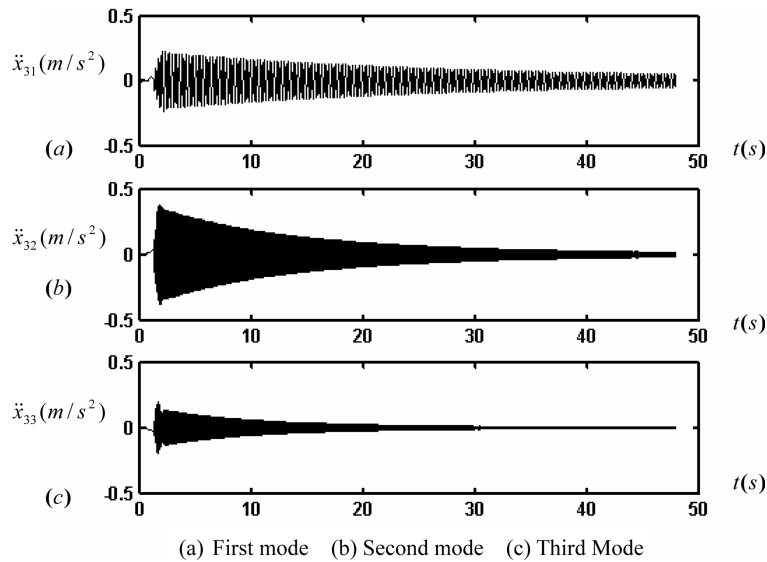


Fig. 4 Modal responses obtained by EMD of the baseline structure

$\ddot{x}_{3j}$ , ( $j = 1, 2, 3$ ). It should be noted that the band-pass filter used should have as small a phase shift as possible. The same modal responses with slight difference at a small segment near  $t = 0$  could be extract from other two acceleration responses  $\ddot{x}_1$  and  $\ddot{x}_2$ .

After removing a small segment near  $t = 0$ , the Hilbert transform was applied to modal acceleration responses as illustrated in Fig. 4 to obtain the corresponding instantaneous amplitudes in the natural logarithm scale and phase angles. Linear least-square fit procedures were used to fit the  $\ln$  amplitudes and phase angles. The  $\ln$  amplitude and phase angle of the first modal response as functions of time  $t$  are shown in Fig. 5 as dotted curves. Also presented in Fig. 5 as solid straight lines are the linear least-square fits. From the slopes of these straight lines, the first mode frequency and damping ratio have been estimated. Repeating the same procedures for other two modal responses, as shown in Fig. 6 and Fig. 7, all the natural frequencies and damping ratios can be obtained from one measurement  $\ddot{x}_3$ . Table 1

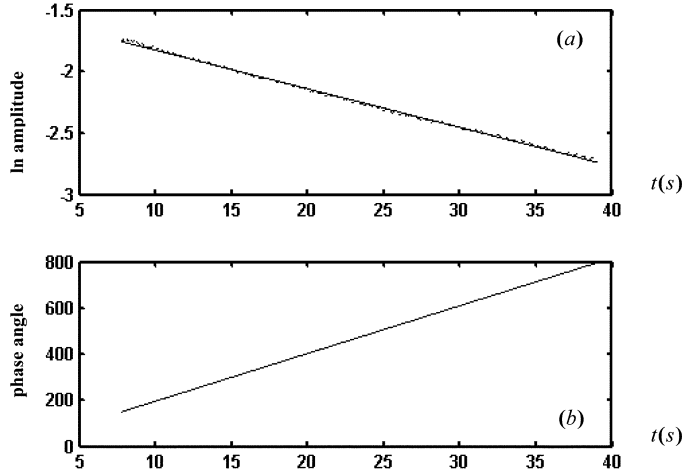


Fig. 5 Plots of ln amplitude and phase angle for the first mode of the baseline structure

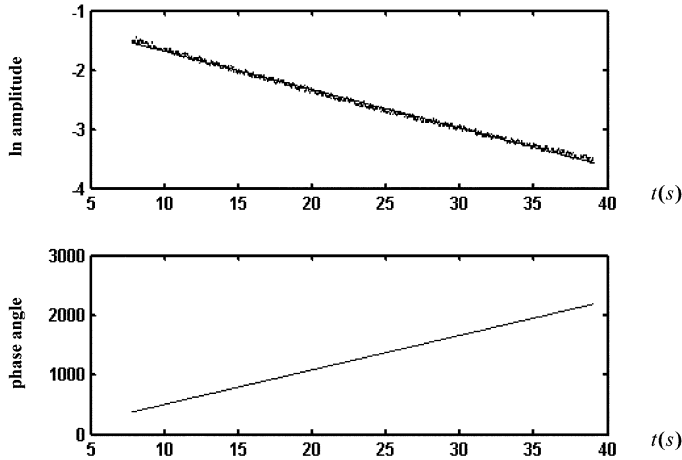


Fig. 6 Plots of ln amplitude and phase angle for the second mode of the baseline structure

presents the identified values of the natural frequencies and damping ratios of the un-damaged (baseline) structure based on a single measurement. Also presented in the table are the FEM results. By comparison, it can be observed that the identified natural frequencies and damping ratios using the HHT method are quite consistent with the FEM results. Similar results have been obtained using other two measured acceleration responses  $\ddot{x}_1$  and  $\ddot{x}_2$ . Table 2 presents the natural frequencies and damping ratios of the baseline structure identified from different responses by HHT. It can be seen that the identified results from different measurements are almost the same.

After repeating the above procedures for the responses at all the three DOFs, the complex mode shapes can be identified by using Eqs. (23)~(26). Further, the physical mass, stiffness and damping matrices were all identified. Table 3 presents the identified modal vectors of the baseline structure by the HHT method. Table 4 shows the identified values for mass, stiffness and damping matrices. The FEM results are also presented in these tables for comparison.

For the two damage patterns considered, the identification procedures are the same as that for the

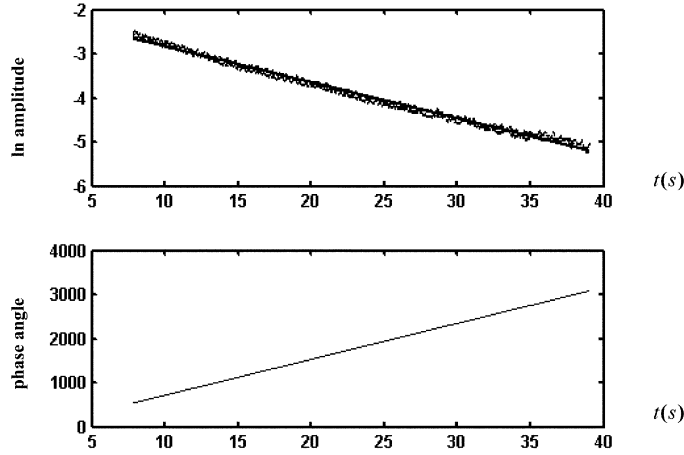


Fig. 7 Plots of ln amplitude and phase angle for the third mode of the baseline structure

Table 1 Comparison of natural frequencies and damping ratios of the baseline structure by FEM and HHT

Mode	FEM		Identified (HHT)	
	Natural Frequency (Hz)	Damping Ratio (%)	Natural Frequency (Hz)	Damping Ratio (%)
1st	3.256	NA	3.295	0.15
2nd	9.101	NA	9.216	0.11
3rd	13.123	NA	12.997	0.10

Table 2 Natural frequencies and damping ratios of the baseline structure identified from different responses by HHT

Mode	$\ddot{x}_1(t)$		$\ddot{x}_2(t)$		$\ddot{x}_3(t)$	
	Natural Frequency (Hz)	Damping Ratio (%)	Natural Frequency (Hz)	Damping Ratio (%)	Natural Frequency (Hz)	Damping Ratio (%)
1st	3.295	0.15	3.295	0.15	3.295	0.15
2nd	9.216	0.10	9.216	0.11	9.216	0.11
3rd	12.995	0.10	12.999	0.10	12.997	0.10

Table 3 Comparison of modal vectors of the baseline structure by FEM and HHT

	Amplitude of modal vector			Phase angle of modal vector (rad)		
	1.00	1.00	1.00			
FEM	1.81	0.45	1.25	NA		
	2.26	0.80	0.55			
	1.00	1.00	1.00	0.00	0.00	0.00
Identified (HHT)	1.93	0.51	1.06	0.00	0.01	-3.14
	2.51	0.79	0.49	0.00	-3.13	-0.01

baseline structure. Table 5 to Table 7 present the identified results for damage pattern I, and Table 8 to Table 10 present the identified results for damage pattern II. From these tables, it is observed that, similar to the results presented in Table 1, Table 3 and Table 4, the identified results for damaged structures are quite reasonable compared with the FEM results.

Table 4 Comparison of mass, stiffness and damping matrices of the baseline structure by FEM and HHT

	Mass (kg)			Stiffness (N/m)			Damping (Ns/m)		
FEM	21.53	0.00	0.00	95238	-47619	0			
	0.00	21.53	0.00	-47619	95238	-47619		NA	
	0.00	0.00	21.53	0	-47619	47619			
Identified (HHT)	19.26	-0.46	-0.67	86161	-40744	-72	4.06	-2.08	-1.73
	-0.46	20.29	-1.48	-40744	85015	-43320	-2.08	2.71	0.72
	-0.67	1.48	18.62	-72	-43320	40810	-1.73	0.72	1.44

Table 5 Comparison of natural frequencies and damping ratios of damage pattern I by FEM and HHT

Mode	FEM		Identified (HHT)	
	Natural Frequency (Hz)	Damping Ratio (%)	Natural Frequency (Hz)	Damping Ratio (%)
1st	3.180	NA	3.206	0.15
2nd	8.055	NA	8.065	0.14
3rd	12.485	NA	12.461	0.10

Table 6 Comparison of modal vectors of damage pattern I by FEM and HHT

	Amplitude of modal vector			Phase angle of modal vector (rad)		
FEM	1.00	1.00	1.00			
	1.81	0.79	0.94		NA	
	2.52	0.96	0.27			
Identified (HHT)	1.00	1.00	1.00	0.00	0.00	0.00
	1.94	0.89	0.79	0.00	0.02	3.14
	2.87	0.98	0.23	0.08	-3.14	0.01

Table 7 Comparison of mass, stiffness and damping matrices of damage pattern I by FEM and HHT

	Mass (kg)			Stiffness (N/m)			Damping (Ns/m)		
FEM	21.53	0.00	0.00	95238	-47619	0			
	0.00	21.53	0.00	-47619	79365	-31746		NA	
	0.00	0.00	21.53	0	-31746	31756			
Identified (HHT)	21.07	-0.52	-0.26	91826	-43227	-288	4.29	-6.58	-5.83
	-0.52	22.41	-1.47	-43227	70480	-26583	-6.58	14.72	12.46
	-0.26	-1.47	19.73	-288	-26583	28961	-5.83	12.46	44.8

From the identified stiffness matrices, the stiffness of each story unit can be identified. Then the damage location and severity can be determined by comparing the stiffness of each story unit before and after the damage. Table 11 presents the identified and FEM results for the stiffness of each story unit for the undamaged structure and damage patterns I and II. In Table 11,  $K_j$  represents the stiffness of  $j$ th story unit, which is numbered from the bottom to the top. From the identified results, it is observed that, in comparison with the baseline structure, damage pattern I results in about 1/3 of the stiffness loss in the third story unit, and damage pattern II results in about 1/3 of the stiffness loss in both the second and third story units. The identified results correlate quite well with the actual stiffness loss in the experimental structures. Thus the damage location and damage severity are identified, and the results are quite satisfactory.

Table 8 Comparison of natural frequencies and damping ratios of damage pattern II by FEM and HHT

Mode	FEM		Identified (HHT)	
	Natural Frequency (Hz)	Damping Ratio (%)	Natural Frequency (Hz)	Damping Ratio (%)
1st	2.946	NA	2.911	0.16
2nd	8.038	NA	8.055	0.12
3rd	11.102	NA	10.988	0.11

Table 9 Comparison of modal vectors of damage pattern II by FEM and HHT

	Amplitude of modal vector			Phase angle of modal vector (rad)		
FEM	1.00	1.00	1.00			
	2.26	0.69	0.96		NA	
	2.97	0.86	0.39			
Identified (HHT)	1.00	1.00	1.00	0.00	0.00	0.00
	2.56	0.84	0.77	0.00	0.01	3.14
	3.53	0.93	0.31	0.12	-3.14	0.01

Table 10 Comparison of mass, stiffness and damping matrices of damage pattern II by FEM and HHT

	Mass (kg)			Stiffness (N/m)			Damping (Ns/m)		
FEM	21.53	0.00	0.00	79365	-31746	0			
	0.00	21.53	0.00	-31746	63593	-31847		NA	
	0.00	0.00	21.53	0	-31847	31847			
Identified (HHT)	19.9	-0.44	-0.01	72993	-40744	-677	4.97	15.54	-10.11
	-0.44	21.37	0.86	-25802	51100	-26538	15.54	80.12	19.05
	-0.01	0.86	22.64	-677	-26538	28781	-10.11	19.05	-79.85

Table 11 Comparison of stiffness of each story unit for baseline structure, damage pattern I and damage pattern II by FEM and HHT

Stiffness (N/m)	FEM			Identified (HHT)		
	Baseline Structure	Damage Pattern I	Damage Pattern II	Baseline Structure	Damage Pattern I	Damage Pattern II
K1	47619	47619	47619	43211	49118	49553
K2	47619	47619	31746	42950	42708	23440
K3	47619	31746	31746	42065	28772	27660

#### 4. Conclusions

This paper presents an experimental study for the system identification and damage detection based on the HHT method. A MDOF structural model has been constructed with modular members to simulate damages at different locations with different severities. Two damage patterns have been considered in the experimental study. Our experimental study demonstrates that the HHT method is capable of accurately identifying the system parameters as well as the location and severity damages. As the result, the HHT method is a promising technique for structural health monitoring.

## Acknowledgements

This research is supported by the National Natural Science Foundation of China under Grant No. 50478037 and No. 10572058, by the Science Foundation of Aeronautics of China under Grant No. 04I52063, and by the National Science Foundation under Grant No. CMS-0220027-01. The financial support is greatly appreciated. The authors are grateful to Professor J. N. Yang of the University of California at Irvine for valuable guidance.

## References

- Chang, F.-K. (ed.) (1997, 1999, 2001, 2003), *Proceedings of 1<sup>st</sup>, 2<sup>nd</sup>, 3<sup>rd</sup> and 4<sup>th</sup> International Workshop on Structural Health Monitoring*, Stanford University, Stanford, CA.
- Doebling, S. W., Farrar, C. R., Prime, M. B. and Shevitz D. W. (1996), "Damage identification and health monitoring of structural and mechanical systems from changes in their characteristics: a literature review", *Report LA-13070-MS*, Los Alamos National Laboratory, Los Alamos, NM.
- Dyke, S. J., Caicedo, J. M. and Johnson, E. (2000), "Monitoring of a benchmark structure for damage identification", *Proceedings of 14<sup>th</sup> ASCE Engineering Mechanics Conference*, Austin, TX.
- Feldman, M. (1994), "Non-linear system vibration analysis using Hilbert transform—I: free vibration analysis method FREEVIB", *Mechanical Systems and Signal Processing*, **8**(2), 119-127.
- Feldman, M. (1997), "Nonlinear free-vibration identification via the Hilbert transform", *J. Sound Vib.*, **208**(3), 475-489.
- Gurley, K. and Kareem A. (1999), "Application of wavelet transform in earthquake, wind, and ocean engineering", *J. Eng. Struct.*, **21**, 149-167.
- Hou, Z., Noori, M. and Amand, R. S. (2000), "Wavelet-based approach for structural damage detection", *J. Eng. Mech.*, ASCE, **126**(7), 677-683.
- Housner, G. W., Bergman, L. A., Garghey, T. K. *et al.* (1997), "Structural control: past, present and future". *J. Eng. Mech.: Special Issue*, ASCE, **123**(9), 897-958.
- Huang, N. E., Shen, Z., Long, S. R., Wu, M. C., Shih, H. H. *et al.* (1998), "The empirical mode decomposition and Hilbert spectrum for nonlinear and nonstationary time series analysis", *Proceedings of the Royal Society of London, Series A*, **454**, 903-995.
- Huang, N. E., Shen, Z. and Long, S. R. (1999), "A new view of nonlinear water waves: the Hilbert spectrum", *Annual Review of Fluid Mech.*, **31**, 417-457.
- Ruzzene, M., Fasana, A., Baribaldi, L. *et al.* (1997), "Natural frequencies and damping identification using wavelet transform: application to real data", *Mechanical Systems and Signal Processing*, **11**(2), 207-218.
- Staszewski, W. J. (1997), "Identification of damping in MDOF systems using time-scale decomposition", *J. Sound Vib.*, **203**(2), 283-305.
- Yang, J. N. and Lei, Y. (1999), "Identification of natural frequencies and damping ratios of linear structures via Hilbert transform and empirical mode decomposition", *Proceedings of the IASTED International Conference on Intelligent Systems and Control*, Santa Barbara, CA.
- Yang, J. N., and Lei, Y. (2000), "Identification of civil structures with non-proportional damping", *Proceedings of SPIE, Smart Structures and Materials*, Newport Beach, CA.
- Yang, J. N., Lei, Y. and Huang, N. (2001), "Damage identification of civil engineering structures using Hilbert-Huang transform", *Proceedings of 3<sup>rd</sup> International Workshop on Structural Health Monitoring*, Stanford University, Stanford, CA.
- Yang, J. N., Lin, S. and Pan, S. (2002), "Damage identification of structures using Hilbert-Huang spectral analysis", *Proceedings of 15<sup>th</sup> ASCE Engineering Mechanics Conference*, Columbia University, New York, NY.
- Yang, J. N., Lei, Y. and Huang, N. (2003a), "Identification of linear structures based on Hilbert-Huang spectral analysis. Part I: normal modes", *J. Earthq. Eng. Struct. Dyn.*, **32**, 1443-1467.
- Yang, J. N., Lei, Y. and Huang, N. (2003b), "Identification of linear structures based on Hilbert-Huang spectral analysis. Part II: complex modes", *J. Earthq. Eng. Struct. Dyn.*, **32**, 1533-1554.
- Yang, J. N., Lei, Y., Lin, S. and Huang N. (2004), "Hilbert-Huang based approach for structural damage detection", *J. Eng. Mech.*, ASCE, **130**(1), 85-95.